

# Mechanical characterization of composite solid rocket propellant based on hydroxy-terminated polybutadiene

Nikola I. Gligorijević, Vesna Ž. Rodić, Saša Ž. Živković, Bojan M. Pavković, Momčilo M. Nikolić, Stevan M. Kozomara, Sredoje D. Subotić

Military Technical Institute, Belgrade, Serbia

## Abstract

This paper presents the procedure of uniaxial mechanical characterization of composite solid rocket propellant based on hydroxy-terminated polybutadiene (HTPB), whose mechanical properties strongly depend on temperature, strain rate, natural aging and accumulated damage. A method of processing data is presented in order to determine time-temperature shift factor and master curves for tensile strength, ultimate strain and relaxation modulus, depending on reduced time. Functional dependences of these features represent an input for structural analysis of a rocket motor propellant grain. The effects of natural aging on the mechanical properties are also considered.

**Keywords:** composite propellant, viscoelasticity, mechanical characterization, tensile strength, ultimate strain, time-temperature shift factor, relaxation modulus, safety factor, reduced time.

Available online at the Journal website: <http://www.ache.org.rs/HI/>

SCIENTIFIC PAPER

UDC 662.1/.4:62:547

Hem. Ind. 70 (5) 581–594 (2016)

doi: 10.2298/HEMIND150217067G

Elastomeric materials have been incorporated as structural elements in many engineering applications. One of their important applications is for design of solid propellant grains in rocket motors.

There are two main types of solid rocket propellants, double-base and composite. Double-base propellant is composed as approximately equal-part mixture of nitrocellulose gelled by a nitrate ester such as nitroglycerin, which depends upon the nitro chemical groups in the nitrocellulose and nitrate ester for oxygen. Composite propellant is composed as a mixture of approximately 75–85% of fine oxidizer powder embedded into the remaining 15–25% of polymer matrix [1–3]. In both cases the elastomeric content is sufficiently large to cause the mixture to exhibit strong strain rate- and temperature-dependent mechanical properties [4].

For elastic materials, in the field of small strains and one-dimensional tension, there is a linear relation between stress ( $\sigma$ ) and strain ( $\varepsilon$ ), which can be compared to behavior of a spring:

$$\sigma = E\varepsilon \quad (1)$$

$E$  – Young's modulus of elasticity.

Viscoelastic mechanical behavior is something between the behavior of elastic spring and viscous fluid. For viscoelastic materials, this relationship is not linear. It depends on strain rate and temperature [5–7].

The relation between the two usually can be presented by a complex differential equation. Under certain assumptions, the viscoelastic material may be treated as linear-viscoelastic material [1,8,9], which is represented by following expression:

$$\begin{aligned} \left[ P_n \frac{d^n}{dt^n} + \dots + P_1 \frac{d}{dt} + P_0 \right] \sigma(t) = \\ = \left[ Q_m \frac{d^m}{dt^m} + \dots + Q_1 \frac{d}{dt} + Q_0 \right] \varepsilon(t) \end{aligned} \quad (2)$$

or more compactly:

$$[O_1] \sigma(t) = [O_2] \varepsilon(t) \quad (3)$$

where  $O_1$  and  $O_2$  are differential operators. Linear operator  $d^i/dt^i$  represents the  $i$ -th derivative with respect to time;  $P_i$  and  $Q_i$  are material constants which may be obtained by uniaxial tension tests. Although the Eq. (2) is complex, if the mechanical properties of material are known, depending on temperature and time, it is theoretically possible to conduct structural analysis by means of mathematical transformations and principles of elastic analysis [1,4,6,7].

Mechanical behavior of any material depends on temperature range in which it is going to be used. All materials behave as elastic below their glass transition temperatures ( $T_g$ ). For instance, if we introduce an analogy between  $T_g$  for elastomers and the high temperature above which the metals become plastic, we can explain the elastic metals behavior at ambient temperature. For their structural analysis the expression (1) is widely used in the theory of elasticity.

Correspondence: N.I. Gligorijević, Military Technical Institute, Ratka Resanovića 1, 11000 Belgrade, Serbia.  
E-mail: nikola.gligorijevic@gmail.com  
Paper received: 17 February, 2015  
Paper accepted: 13 November, 2015

The value of  $T_g$  is the first feature that should be determined in the process of mechanical characterization of a composite propellant composition based on a certain type of polymer (such as HTPB). The glass transition temperature  $T_g$  of the composite solid propellant composition, based on HTPB, which is discussed in this paper is approximately equal to  $-70\text{ }^\circ\text{C}$  [10,11].

The composite rocket propellant, based on HTPB, is viscoelastic over its glass transition temperature  $T_g$  in its operational temperature range between  $-40$  and  $50\text{ }^\circ\text{C}$ .

All of its mechanical properties vary with temperature, real time due to aging, and significantly with strain rate which is also a kind of a time dependence.

For this reason, it is necessary to conduct mechanical characterization of viscoelastic material in order to get all the dependences, necessary to improve a reliable structural analysis which substantially differs from the analysis for elastic materials. Usually, the structural analysis is based on uniaxial mechanical characterization.

The purpose of mechanical characterization of the viscoelastic rocket propellant is to conduct the structural analysis for a rocket propellant grain as viscoelastic body and to assess the time-distribution of the safety factor, or more generally, to determine the reliability of the rocket motor. The safety factor is the ratio between tensile strength and real stress that acts on a body, or between ultimate and real strain:

$$v_\sigma(t) = \frac{\sigma_m(t)}{\sigma(t)}; v_\varepsilon(t) = \frac{\varepsilon_m(t)}{\varepsilon(t)} \quad (4)$$

Real stresses and strains depend on the loads that act on the body, but also on environmental temperature and relaxation modulus [1,5–7] of the material.

$$\sigma, \varepsilon = f(T, E_{rel}(t)) \quad (5)$$

From the Eqs. (4) and (5) it can be seen that it is necessary to determine the three main dependencies:  $\sigma_m(T, t)$ ,  $\varepsilon_m(T, t)$  and  $E_{rel}(T, t)$ . The first two, tensile strength and ultimate strain are required for failure analysis, and the third, relaxation modulus, for the real stress and strain calculations.

According to Heller's model [10,12,13], each of these features is a combination of basic values in the very beginning of the propellant service life ( $\sigma_{m0}, \varepsilon_{m0}, E_{m0}$ ), aging factors ( $\eta_\sigma, \eta_\varepsilon, \eta_E$ ) and cumulative damage ( $D$ ) due to load effects during storage.

$$\sigma_m(t) = \sigma_{m0} \eta_\sigma(t) [1 - D(t)] \quad (6)$$

$$\varepsilon_m(t) = \varepsilon_{m0} \eta_\varepsilon(t) [1 - D(t)] \quad (7)$$

$$E_{rel}(t) = E_{rel0} \eta_E(t) [1 - D(t)] \quad (8)$$

There are different opinions on how to describe the changes of the mechanical properties of viscoelastic

materials during time. Sutton [14], for instance, suggests that changes occur only due to the effects of load and he doesn't consider the effects of natural aging ( $\eta_\sigma, \eta_\varepsilon, \eta_E$ ). He finds that changes in mechanical properties are primarily due to cumulative damage ( $D$ ) [11,14–17]. Sometimes, propellant aging is considered as a unique result of simultaneous action of chemical, physical and aging due to the effects of mechanical loads [18]. However, all authors agree that it is necessary to determine the basic initial values of the mechanical properties ( $\sigma_{m0}, \varepsilon_{m0}, E_{m0}$ ), immediately after propellant production. Sometimes for the structural analysis only these values are used, such as there are no further changes due to aging.

The basic values of mechanical properties ( $\sigma_{m0}, \varepsilon_{m0}, E_{m0}$ ) are formally represented in Eqs. (6–8) as constants. Really, these features are variables, that depend on temperature and strain rate, usually presented in the form of master curves [1,5–7,19]. There are several convenient tests for the mechanical characterization of viscoelastic material. It is customary to test uniaxial specimens in tension. Four tests are commonly used [1,6,19]:

1. Step-strain input, measure stress-relaxation output,
2. Step-stress input, measure creep-strain output,
3. Constant strain-rate input, measure stress output and
4. Sinusoidal stress (strain) input, measure strain (stress) output.

In practice, the most commonly used test is constant strain-rate test (No. 3) because data processing is similar to the processing the test results made by elastic materials. For a discussion of cyclic loads, the test No. 4 is also very useful.

Usually, in the literature, only the principles for determination of viscoelastic mechanical properties can be found. The main goal of this paper is to present the complete procedure of the composite solid propellant characterization and determination of the master curves for tensile strength, allowable strain and relaxation modulus. These features are used as an input in the process of structural analysis of the propellant grain in rocket motor and its reliability estimation. Moreover, the possibility of application these results after a certain period of propellant storage was analysed [10,19].

## EXPERIMENTS

### Composite propellant composition and preparation of test samples

A composite solid propellant composition based on hydroxy-terminated polybutadiene (HTPB) has been tested [20], composed by 23,4% HTPB based binder,

75% crystalline oxidizer (ammonium perchlorate, AP), 1% Al metal powder, 0,5% lithium fluoride as burning rate depressant and 0,1% carbon black powder (C) as burning stabilizer. Within the HTPB based binder, isophorone diisocyanate (IPDI) as curing agent (cross-linker) was used, as well as dioctyl adipate (DOA) as plasticizer, 2,2-methylene-bis(4-methyl-6-tertiary-butyl phenol) (AO22) as antioxidant and triethylene-tetra-mine (TET), as bonding agent.

The NCO/OH ratio between the isocyanate groups of IPDI to the hydroxy groups was 0.86.

During propellant grain manufacturing, propellant blocks were also cast and placed into a dry environment at 20 °C. The specimens were cut from the blocks immediately before daily series testing. The remaining blocks were returned to thermally controlled dry stock. Thus, external loads or other forms of damage didn't affect the propellant blocks.

For uniaxial constant strain-rate tests and stress–strain curves measuring, tensile tester “Instron-1122” was used.

Propellant specimens are usually tempered in small separated thermal chambers with constant temperatures for at least two hours before tension test. The same temperature is also prepared in the main chamber on the Instron tester (Fig. 1). When the test temperature has to be low, the main chamber is cooled by liquid CO<sub>2</sub>. Before test, each individual specimen is transferred into a chamber on the testing machine, with further tempering until the desired temperature is stabilized.

In Fig. 1 it can be seen that the height of the chamber is large enough to enable movement of the tensile tester cross-head, which is higher than the maximum strain of the specimen.



Figure 1. Tensile tester „Instron-1122“.

When the temperature chamber is not mounted on the tester, the values of real strain on standard (room) temperature can be measured by extension-meter.

When the tests have to be performed at other temperatures, using temperature chamber, it is not possible to mount extension-meter. However, for JANNAF-C specimen the effective gauge length of  $l_0 = 68.4$  mm has been widely adopted in the literature [1,6,7,16]. Our tests on standard temperature have shown strong agreement between strain measured by extension-meters and strain based on the displacement of the tester cross-head and effective gauge length.

Two sets of tension tests have been made. At first, fresh, virgin propellant was tested, immediately after curing, in order to make master curves for the characteristic mechanical properties. Propellant specimens of the “JANNAF-C” type [6,8] were tested in 96 different modes, under various temperature and strain rate conditions (Table 1), with 7–9 replicates in each mode. Twelve different temperatures and twelve different strain rates were used (ten degree steps in the range –60 to 50 °C), constant crosshead speeds between 0.2 and 1000 mm/min. The influence of time as a result of strain rate was analyzed.

In contrast to the first, in the second group of tests the impact of real-time on the mechanical properties was analyzed, having regard to the natural aging. The propellant was tested in two different periods. For the first time, 15 days after production, and for the second time, about three months later. The tests were carried out only at standard temperature (20 °C), at several different cross-head speeds.

The procedure in the first set of tests [1,4–7,11] was as follows: at the initial, constant temperature (*i.e.*, –60 °C in the left column in Table 1), uniaxial tension tests were performed at several different tester cross-head speeds (*i.e.*, 5, 10, 20, 50, 100, 200, 500 and 1000 mm/min). Then, the procedure has been continued at the next temperature –50 °C. And so on, until the testing has been completed at the upper limit temperature, 50 °C.

Table 1. Test modes of uni-axial tension; R – crosshead speed

R mm/min	T / °C												
	–60	–50	–40	–30	–20	–10	0	10	20	30	40	50	
1000	*	*	*	*									
500	*	*	*	*	*	*	*	*					
200	*	*	*	*	*	*	*	*	*	*	*	*	*
100	*	*	*	*	*	*	*	*	*	*	*	*	*
50	*	*	*	*	*	*	*	*	*	*	*	*	*
20	*	*	*	*	*	*	*	*	*	*	*	*	*
10	*	*		*	*	*	*	*	*	*	*	*	*
5	*	*				*	*	*	*	*	*	*	*
2							*	*	*	*	*	*	*
1								*	*	*	*	*	*
0.5									*	*	*	*	*
0.2											*	*	*

Three characteristic mechanical properties (Fig. 2) were determined in each single test: the initial modulus ( $E$ ), the maximum allowable stress, termed tensile strength ( $\sigma_m$ ) and the strain at maximum stress ( $\epsilon_m$ ). At some temperatures there was no need to carry out tests at all different cross-head speeds. The number of test modes for each test temperature was less or equal to the number of possible tester speeds (strain rates). Each individual stress-strain test, as a combination of strain rate and test temperature, have given only three values, one point for each of the three summary property plots: initial modulus, tensile strength and strain at maximum stress (ultimate strain).

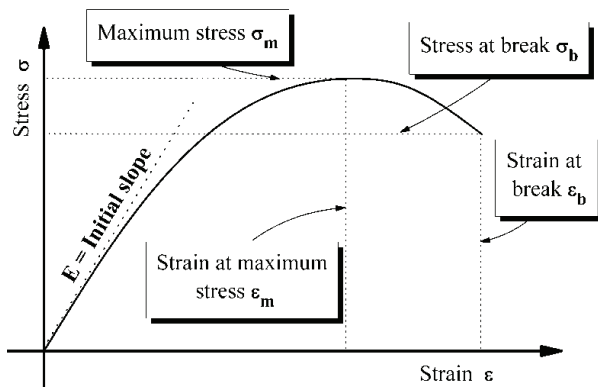


Figure 2. Typical stress-strain curve in the constant strain-rate test.

In the second group of tests, uniaxial tension tests were carried out, not in the very beginning of the service life, like the first series of tests, but still in the initial period after production, the first time after 15 days and the second time 105 days after curing. Both times, the second group of tests was performed only at standard temperature (20 °C), at nine different cross-head speeds: 0.5, 1, 2, 5, 10, 20, 50, 100 and 200 mm/min. The measured values for all three characteristic mechanical properties ( $\sigma_m$ ,  $\epsilon_m$  and  $E$ ) are shown in Table 2.

Table 2. Coefficients that define regression for relaxation modulus master curve

$i$	1	2	3	4	5	6	7
$\tau_i / s$	$10^{-7}$	$10^{-6}$	$10^{-5}$	$10^{-4}$	$10^{-3}$	$10^{-2}$	$10^{-1}$
$E_i$ daN cm <sup>-2</sup>	10.50	40.82	149.61	108.65	139.54	55.56	65.97
$i$	8	9	10	11	12	13	
$\tau_i / s$	$10^0$	$10^1$	$10^2$	$10^3$	$10^4$	$10^5$	
$E_i$ daN cm <sup>-2</sup>	35.31	40.12	14.29	17.90	4.24	1.14	
$E_e$ daN cm <sup>-2</sup>	36.31						

### Test method

The JANNAF specimen, conditioned at a constant temperature, is extended at a constant cross-head speed ( $V$ ) until it breaks. The strain rate ( $\dot{\epsilon}$ ) is also a constant value, commonly denoted as  $R$ . For this type of specimen the value of  $l_0 = 68.4$  mm is used as effective specimen length [6]. The value of force at the extended length is measured as time progresses.

The following values for analysis are defined.

Strain at time  $t$ :

$$\epsilon = \frac{V}{l_0} t = \dot{\epsilon} t \tag{9}$$

True stress:

$$\sigma = \frac{F(1+\epsilon)}{A_0} = \frac{F}{A_0} \left(1 + \frac{V}{l_0} t\right) \left(\frac{\text{daN}}{\text{cm}^2}\right) \tag{10}$$

Strain rate:

$$\frac{d\epsilon}{dt} = \dot{\epsilon} (s^{-1}) = R = \frac{V(\text{mm/min})}{60l_0(\text{mm})} \tag{11}$$

### Processing of measurement results

Each test mode in this type of test gives three values, one for all of the three summary plots. The all three plots ( $\sigma_m$ ,  $\epsilon_m$ ,  $E$ ) should have the same abscissa, which represents reciprocal of the propellant specimen strain rate,  $\log(\dot{\epsilon}^{-1}) = \log(1/R)$ , and have time dimension. The range from the maximum cross-head speed (1000 mm/min) to minimum value (0,2 mm/min) is high, so the logarithmic scale of the abscissa is suitable for further analysis.

For the first series of tests the further procedure was as follows: when all the points were plotted, 96 of them, the regression lines were created for each temperature in all the three material property plots. The procedure was repeated for the entire temperature range from -60 to 50 °C, at ten-degree increments.

Whenever it is necessary to make a plot of a feature that depends on temperature, the reference temperature, denoted as  $T_R$  or  $T_0$  has to be arbitrarily chosen. Standard value ( $T_0 = 20$  °C) is usually recommended [6,7,21,22], although there are cases where it is better to adopt a value about 50 °C over the glass-transition temperature [5]. Since the elastic forces in polymers are proportional to absolute temperature [1,5,6], tensile strength and initial modulus have to be normalized by factor ( $T_0 / T$ ). The initial modulus dependence on temperature and strain rate is shown in Fig. 3.

Similarly, the regression lines for tensile strength vs. strain rate were formed for different test temperatures in the summary plot (Fig. 4). As in the previous plot for the modulus, each temperature dependence was fitted by linear function.

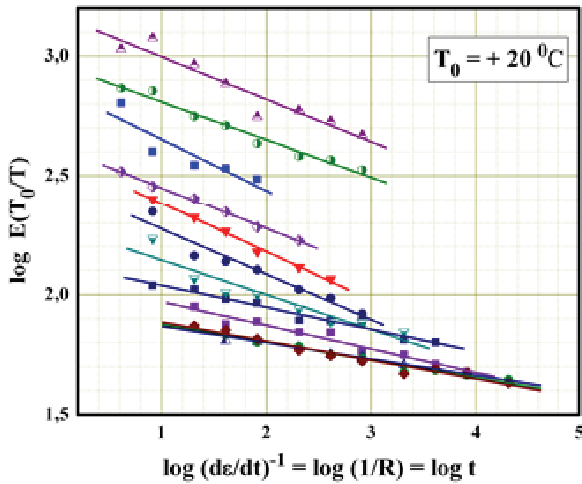


Figure 3. Initial modulus vs. temperature and strain rate.

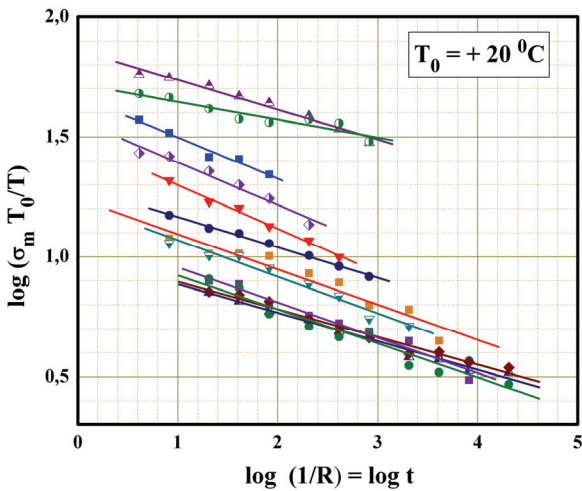


Figure 4. Tensile strength vs. temperature and strain rate.

It can be accepted that the regression lines in Figs. 3 and 4 are approximately linear and parallel. If it is assumed that the hydroxyl-terminated polybutadiene HTPB is a linear-viscoelastic and thermo-rheologically simple material [1,4–7,23], then there exists a correlation between the effects of time and temperature. In this case it is possible to translate all the temperature regression lines horizontally along the time-dimensioned abscissa to meet the reference line, where they overlap to create “a master curve”.

Ultimate strain dependence on temperature and strain rate (Figure 5) is more complex and it is not possible immediately to recognize its final form. Regression lines that correspond to different temperatures do not have proper forms. They are not equidistant as in the cases of modulus and tensile strength.

Distance from an arbitrary line in Figs. 3 and 4 to the line that corresponds to a reference temperature ( $T_0$ ) is equal to the value of shift  $\log a_T$ . This feature is known as a time-temperature shift factor, because the

shift from an arbitrary to the reference temperature corresponds to the horizontal shift along the time axis [1,3–9]. Depending on the direction of movement, this value can be positive or negative. The character of time-temperature shift factor  $a_T$  [1,5–7,21,23] is universal and it can be theoretically determined from each of the plots in Figs. 3–5. The final result  $a_T(T)$  should be same. However, it is much easier to estimate different distances between regression lines using linear plots in Figs. 3 and 4.

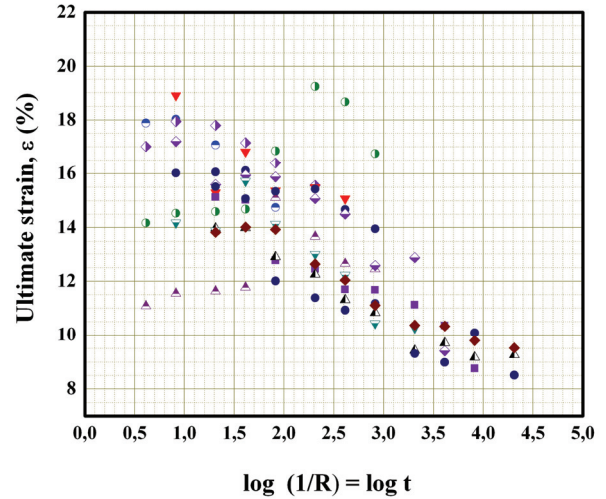


Figure 5. Ultimate strain vs. temperature and strain rate.

Different values of shift correspond to each temperature. When the regression lines are not completely parallel, the distance is determined as in Fig. 6. This way, the functional dependence  $a_T(T)$  between time and temperature can be defined, as in Fig. 7.

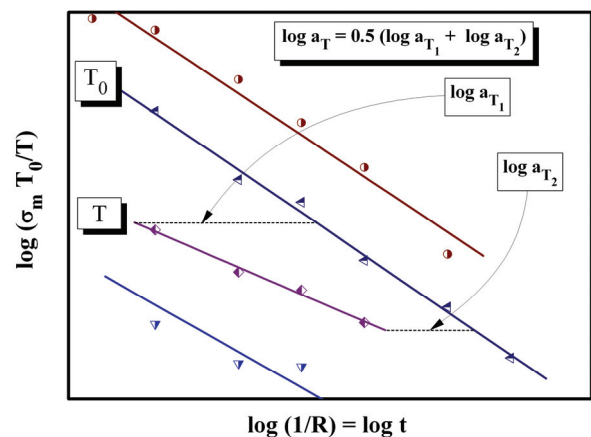


Figure 6. Shift factor  $a_T$  - spacing between regression curves.

Regression line that describes the time-temperature dependence can be described in different ways. In



literature, the most commonly used term is Williams-Landel-Ferry (WLF) Equation:

$$\log a_T = -\frac{C_1(T - T_0)}{C_2 + T - T_0} \tag{12}$$

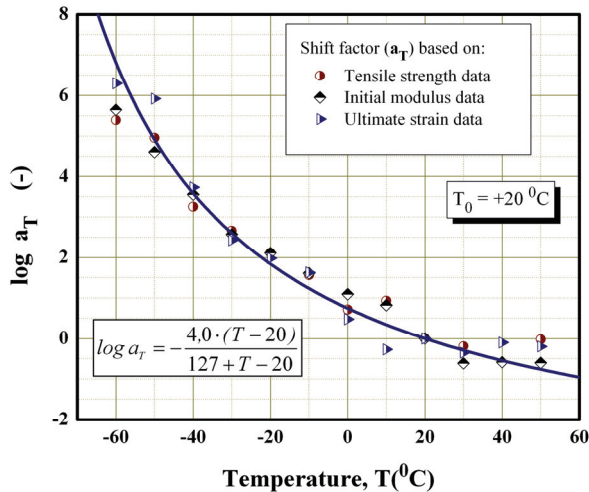


Figure 7. Time-temperature shift factor.

The functional dependence (12) is found to be the same ( $C_1 = 8.86$ ,  $C_2 = 101.6$ ) for a “wide variety of polymers, polymer solutions, organic glass-forming liquids, and inorganic glasses” [24], “after suitable choice of the reference temperature ( $T_0$ ), about 50 °C above the glass transition temperature  $T_g$ , and over the temperature range  $T_0 \pm 50$  °C”. Theoretically, this allows the mechanical properties of some materials to be tested only at one single temperature, and the property values at other temperatures are easy to calculate using the expression (12). However, outside this range, the functional dependences  $a_T(T)$  for different materials cannot match.

Unfortunately, this rule is not entirely suitable for rocket propellants. Composite rocket propellant is a mixture of approximately one quarter of polymer matrix and three quarters of powdered fillers, and expression (12) does not give completely accurate results if the universal constants  $C_1$  and  $C_2$  are used. In addition, the upper limit temperature of propellant usage does not meet the requirement for using these values of constants, because it comes out from the range  $[T_g, T_g + 100$  °C]. For such cases in the same paper [24] it was recommended that “for the practical use, it is more accurate to choose a higher reference temperature ( $T_0$ ) and use the empirical constants of Eq. (12) in predicting the temperature dependence of mechanical properties”. This requires to conduct the propellant mechanical characterization over the entire operating temperature range and to determine the constants in the expression (12) by fitting the test results.

For the specified propellant, the result is shown in section „Data processing results“, together with other results.

The obtained result represents a regression curve on the basis of tensile strength, initial modulus, and allowable strain data. This regression curve refers to the temperature range in which the measurements were made (–60 to 50 °C), and it is quite enough to cover the whole temperature range of the propellant use.

Finally, the scale of the abscissa in the material property plots (Figs. 3–5) can be corrected, because “there exists the fortunate, although essentially unexplained” [4], association between time and temperature for viscoelastic materials. If any of the regression lines on an arbitrary temperature  $T$ , for example  $\sigma_m(T, \log t)$ , is moved for the value  $\log a_T(T)$  to overlap the reference regression line  $\sigma_m(T_0, \log t)$ , this feature begins to depend not only on time but also on the size of displacement along the timeline:

$$\sigma_m(\log t - \log a_T) = \sigma_m(\log t / a_T) = \sigma_m \log \xi$$

Therefore, instead of real time  $t$  which is the reciprocal of the strain rate ( $1/R = t$ ), a “reduced time” ( $\xi$ ) should be introduced on the abscissa ( $\xi = 1/(Ra_T) = t/a_T$ ). This connection between temperature and time is used to transform the dependence on two variables into the dependence on a single variable ( $\log \xi$ ).

Then, the master curve for a given mechanical property may be plotted against  $\log \xi$  that applies to all load conditions. The master curves for tensile strength and initial modulus are of the same type (Figs. 8 and 9):

$$\log \sigma_m \frac{T_0}{T} = a - b \log \xi \tag{13}$$

$$\log E_0 \frac{T_0}{T} = c - d \log \xi \tag{14}$$

A considerable problem in the master curve determination for ultimate strain of the propellant was insufficient recognition (Fig. 5) of individual segments that correspond to different temperatures. Regression curves for these individual segments correspond only to small parts of the final master curve (Figs. 10 and 11) and do not cover the whole time range.

The actual values of the coefficients in linear equations for tensile strength and initial modulus (Eqs. (13) and (14)) are presented in section „Data processing results“, together with other results. For allowable strain the Gaussian regression curve is accepted, in the following form:

$$\varepsilon_m (\%) = \varepsilon_0 + A e^{-2 \left( \frac{\xi - \xi_0}{B} \right)^2} \tag{15}$$

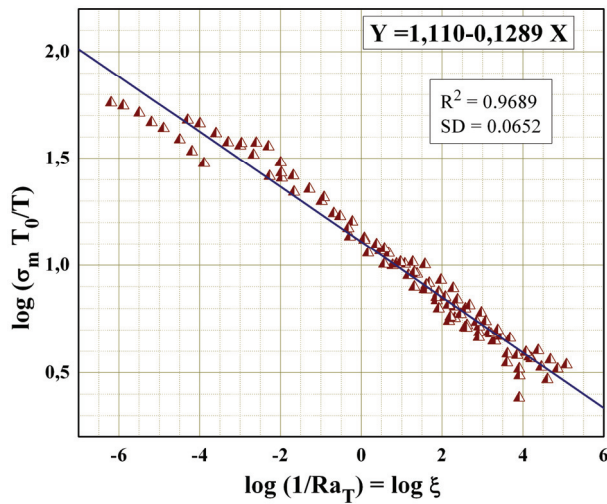


Figure 8. Tensile strength master curve.

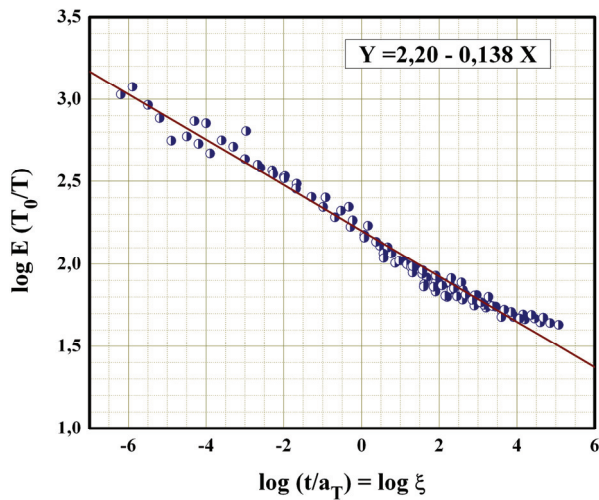


Figure 9. Initial modulus master curve.

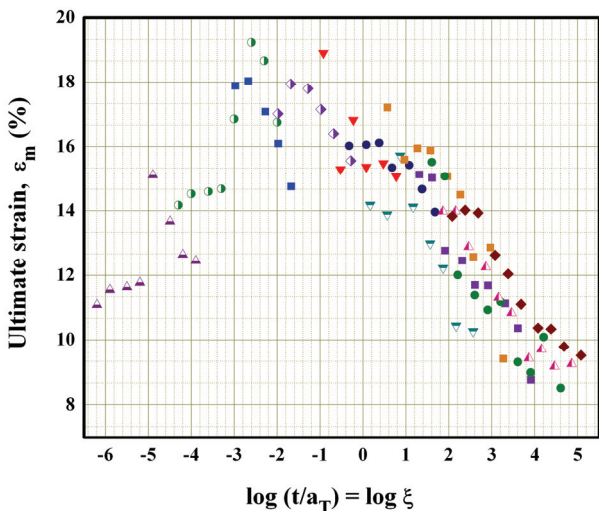


Figure 10. Ultimate strain.

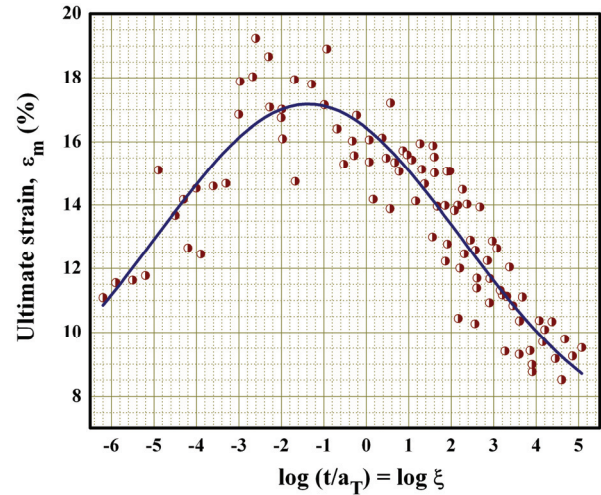


Figure 11. Ultimate strain master curve.

There is no standard form for mathematical description of the ultimate strain curves for different propellant compositions based on HTPB polymer. The Gaussian curve is just an example for an appropriate regression function.

Some individual points in the master plots deviate from the regression lines due to various influences. They are inevitable consequence in the testing of viscoelastic materials. In the probabilistic model [10,11,19], used to estimate a rocket propellant grain reliability, these deviations were compensated because all the features were considered as statistical variables.

Master curves for tensile strength (Fig. 8) and ultimate strain (Fig. 11) are required for failure analysis, as indicators of the material capacity to withstand the loads and stresses.

Before the failure analysis as final stage in the process of reliability determination, the structural analyst has to analyze the stresses acting on the body. For the stress-strain analysis of a viscoelastic body, it is necessary and sufficient to determine the relaxation modulus [1,4,6,9,25–27]. It is very important to make a distinction with respect to the initial modulus of the material which corresponds to the modulus of elasticity in the elastic material.

There are different ways for determination of the relaxation modulus, like DMA tests or long duration relaxation tests. In this study, the relaxation modulus has been determined on the basis of uniaxial constant strain rate tests. Each test mode was sufficient only for one point determination of the master curve, using the following expression [4–7]:

$$E_{rel}(t) = \left[ \frac{d\sigma(t)}{d\varepsilon} \right]_{\varepsilon=Rt} \quad (16)$$

The expression (16) represents the relationship between relaxation modulus and the maximum slope

of the stress-strain curve in the constant strain rate test (Fig. 12), in the domain where the strain is proportional to time ( $\varepsilon = Rt$ ). The maximum slope is approximately equal to the initial modulus which is determined in a known manner, like in the case of an elastic material. In the initial region of the curve that corresponds to its elastic part, two pairs of stress and strain values have to be measured:

$$E_i(t) = \frac{d\sigma(t)}{d\varepsilon} \approx \frac{\Delta\sigma}{\Delta\varepsilon} = \frac{\sigma_2 - \sigma_1}{\varepsilon_2 - \varepsilon_1} \quad (17)$$

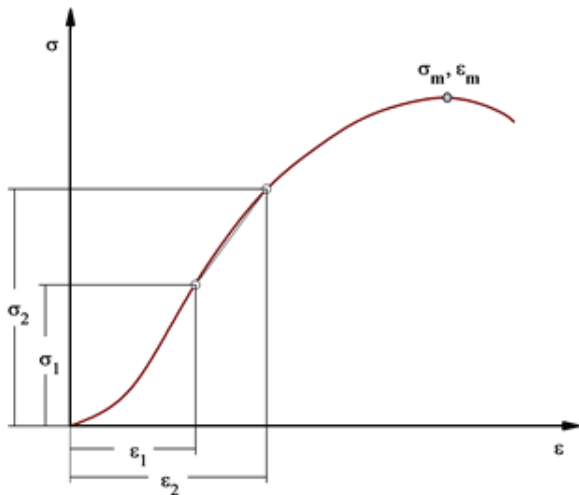


Figure 12. Slope of the stress-strain curve.

It is difficult to determine a rule for measuring the two pairs of stress and strain values. In the paper [28], the authors have measured the values of stress at 3% and 10% strain. However, when the tests are made in a number of different modes, this rule can not be applied.

The method of the relaxation modulus determination is reduced to measuring slopes in different stress-strain test modes. It is important that the value of the relaxation modulus in an exactly defined temperature and speed mode depends not only on the slope of the curve, but also on the position of the measured points on the stress-strain curves ( $\sigma_1, \varepsilon_1, \sigma_2, \varepsilon_2$ ).

Therefore, it is necessary, besides the slope ( $\Delta\sigma/\Delta\varepsilon$ ), to define the position of the measuring points ( $\sigma/\varepsilon$ ) in each stress-strain plot. Therefore, for the relaxation modulus determination, the following procedure has been applied [5,8,9,19]:

$$E_{rel}(t) = \frac{d\sigma}{d\varepsilon} = \frac{\frac{d\sigma}{\sigma}}{\frac{d\varepsilon}{\varepsilon}} \cdot \frac{\sigma}{\varepsilon} = \frac{\sigma}{\varepsilon} \cdot \frac{d(\ln\sigma)}{d(\ln\varepsilon)} \quad (18)$$

The ratio ( $\sigma/\varepsilon$ ) defines the position of the measuring point in the stress-strain diagram. If the influence of strain rate ( $R$ ) and temperature ( $a_T$ ) is int-

roduced, and the stress is normalized ( $T_0/T$ ), an expression for the relaxation modulus is obtained:

$$E_{rel}(t, T) = \frac{\sigma}{\varepsilon} \cdot \frac{d(\ln\sigma)}{d(\ln\varepsilon)} = \frac{\frac{\sigma}{Ra_T} \cdot \frac{T_0}{T} \cdot d\ln\left(\frac{\sigma}{Ra_T} \cdot \frac{T_0}{T}\right)}{\frac{\varepsilon}{Ra_T} \cdot d\ln\left(\frac{\varepsilon}{Ra_T}\right)} \quad (19)$$

$$E_{rel}(t, T) = \frac{\sigma_{RED}}{\varepsilon_{RED}} \cdot \frac{d(\ln\sigma_{RED})}{d(\ln\varepsilon_{RED})} \quad (20)$$

$\sigma_{RED}, \varepsilon_{RED}$  – reduced values of stress and strain.

When the values  $\sigma_{RED}$  and  $\varepsilon_{RED}$  in all stress-strain plots are determined, it is possible to form a log-log plot (Fig. 13), with constant slope, equal to the derivative on the right side of Eq. (20).

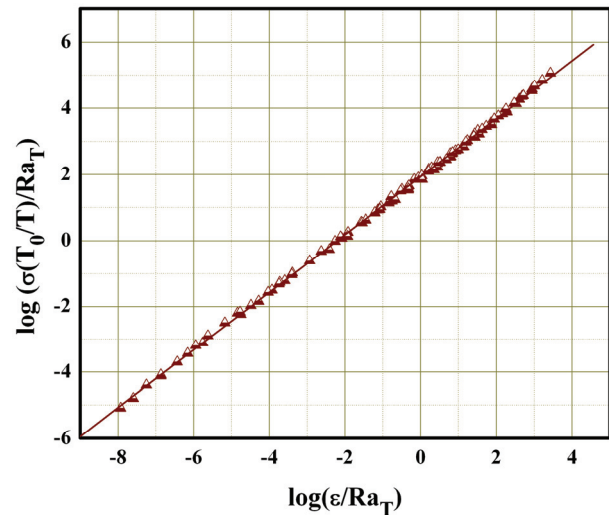


Figure 13. Determination of the relaxation modulus slope.

Finally, it is possible to plot the points defined in Eq. (20). The value  $d(\ln\sigma_{RED})/d(\ln\varepsilon_{RED})$  is approximately constant, but the values of the ratio  $\sigma_{RED}/\varepsilon_{RED}$  are variables, and an array of points can be formed (Fig. 14), determining the relaxation modulus curve [5,6].

The number of 96 different test regimes at various temperatures and cross-head rates was sufficient to produce a reliable relaxation curve covering the whole area that is interesting for structural analysis of a viscoelastic body.

The distribution of the relaxation modulus “master” curve is represented by Dirichlet or Prony series expansion, which is the most general form of linear viscoelasticity:

$$E_{rel}(t) = E_e + \sum_{i=1}^{i=n} E_i e^{-\frac{t}{\tau_i a_T}} \quad (21)$$



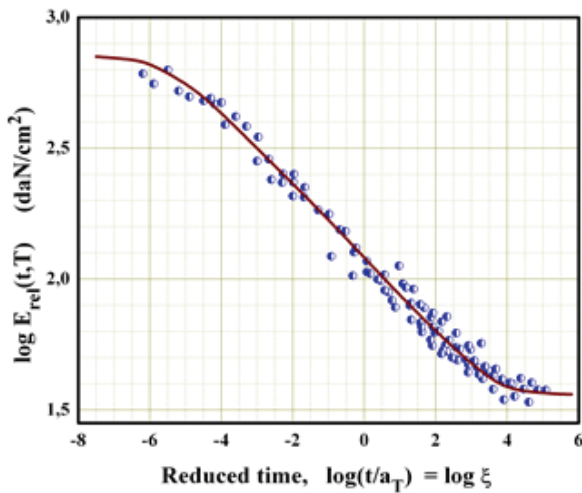


Figure 14. Relaxation modulus.

For the actual HTPB composite propellant, the values of coefficients  $E_i, \tau_i$  (Table 2) are evaluated by fitting the relaxation modulus master curve (Fig. 14) and presented in Section 3, together with other results.

Expression (21) allows the stress and strain analysis to be conducted in all load cases. Generally, in the structural analysis of a viscoelastic body, due to the complex relation between stress and strain, a method is known which translates the problem into the complex domain, where the viscoelastic problem can be solved on the principles of elastic analysis [1,4]. Expression (21) is suitable for the Laplace transform, because the differential relationship between stress and strain in the expressions (2) and (3) turns into a ratio of two polynomials.

For cyclic loads analysis, the frequency-dependent complex modulus is necessary [1,6,7,11]. This feature may be obtained by dynamic mechanical analyzer (DMA). However, it is also possible to convert uniaxial tensile tests data to dynamic data, according to Williams [1,4].

The dynamic modulus takes the form (22) and (23) which is generally known in the theory of viscoelastic materials [1,4–7,12,25]. The values of coefficients are the same as in Eq. (21).

$$E'(\omega) = E_e + \sum_{i=1}^{i=n} \frac{E_i \omega^2 \tau_i^2 \alpha_T^2}{1 + \omega^2 \tau_i^2 \alpha_T^2} \quad (22)$$

$$E''(\omega) = \sum_{i=1}^{i=n} \frac{E_i \omega \tau_i \alpha_T}{1 + \omega^2 \tau_i^2 \alpha_T^2} \quad (23)$$

Good examples of structural integrity analysis under vibration loads can be found in the studies [8,10–13,15,17,19]. The effects of daily and seasonal temperature fluctuations have been discussed, and their impact on the stress-strain field in viscoelastic bodies.

The accumulation of damage in solid propellant rocket grains has also been discussed. A similar approach can be applied to any arbitrary body exposed to cyclic loads.

The second group of tests was carried out in two different periods, only at standard temperature 20 °C, at different strain rates. Based on the tests on nine different cross-head speeds of the tensile tester (0.5, 1, 2, 5, 10, 20, 50, 100 and 200 mm/min), it was possible to form reliable regression curves for the two considered periods.

For each characteristic feature (Initial modulus, tensile strength and Ultimate strain) one diagram has been prepared for both time periods. In all three cases, two different regression lines apply to the same standard temperature and different periods. In Figs. 15–17 the pairs of regression lines are shown for the initial modulus, tensile strength and ultimate strain.

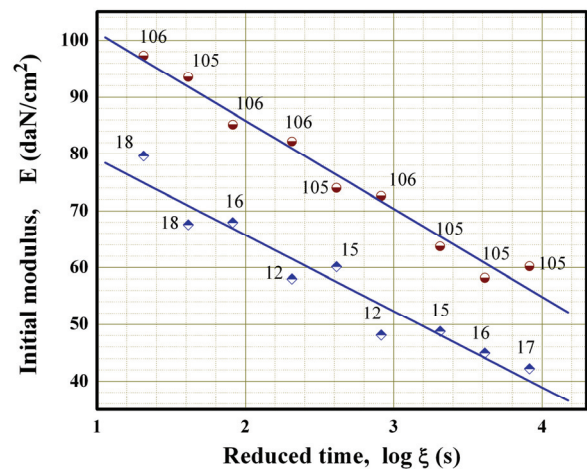


Figure 15. Initial modulus vs. strain rate and aging time.

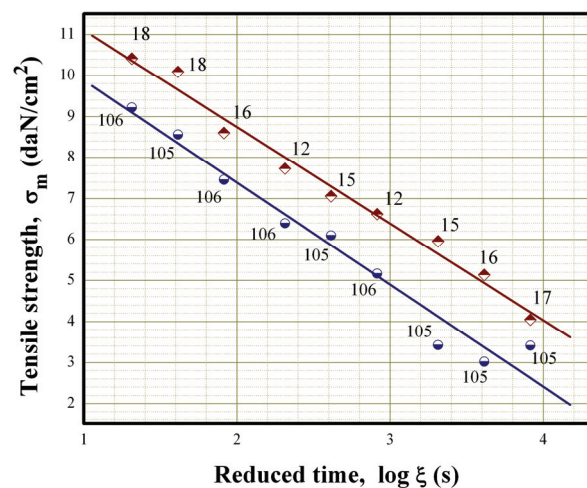


Figure 16. Tensile strength vs. strain rate and aging time.

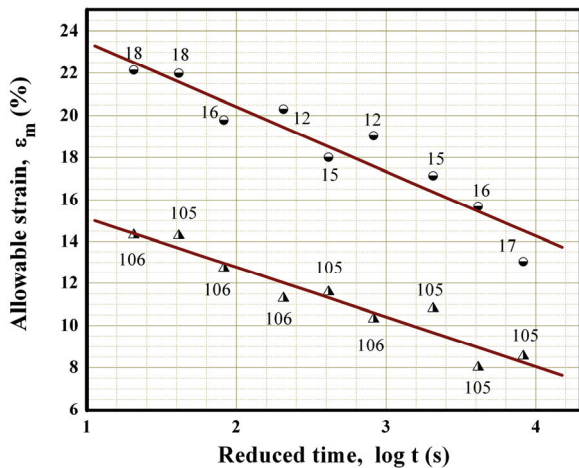


Figure 17. Ultimate strain vs. strain rate and aging time.

**Data processing results**

After the data processing in a manner presented in section „Processing of measurement results“, the results have been prepared in a form that can be used in the structural analysis. Although this study is concerned with composite rocket propellant, which is very specific viscoelastic material, without a wide application in engineering practice, except in missile technology, the results can be used as a basis for structural analysis of similar types of composite materials with polymer matrix.

1. Tensile strength master curve:

$$\log \sigma_m \frac{T_0}{T} = 1,11 - 0,129 \log \left( \frac{t}{a_T} \right) \tag{24}$$

2. Ultimate strain master curve:

$$\varepsilon_m (\%) = 6.663 + 10.514 e^{-2 \left( \frac{\xi + 1.366}{7.119} \right)^2}; \xi = \frac{t}{a_T} \tag{25}$$

3. Time-temperature shift factor >

$$\log a_T = - \frac{4.0(T - 20)}{127 + T - 20} \tag{26}$$

4. Initial modulus master curve:

$$\frac{T_0}{T} \log E = 2.20 - 0.138 \log \left( \frac{t}{a_T} \right)$$

5. Relaxation modulus master curve, Eq. (21); material constants are shown in Table 2.

In the structural analysis of solid propellant rocket grains, the methods of statistics and probability are usually used, in order to determine or estimate reliability and service life [10–13,19,29]. Therefore, it is often necessary to determine the statistical parameters that define these features. In this paper the statistical

parameters of the propellant mechanical properties haven't been considered.

**DISCUSSION**

**Elastic and viscoelastic analysis of safety factor**

The tensile strength of an elastic material is treated in the theory of elasticity as a constant value. In this theory, in simple terms, the safety factor is defined (eq. 4) as the ratio of the tensile strength ( $\sigma_m$ ) to the maximum real equivalent stress ( $\sigma_0$ ), as a resultant of the simultaneous action of different loads.

For a viscoelastic body, the tensile strength depends on temperature and strain rate, and also on the viscoelastic material age and cumulative damage. When two or more loads act on the body in different manners, it is not possible to define the equivalent tensile strength. In addition, the stresses due to applied forces depend on material properties which are also dependent on temperature and strain rate. The need for detailed mechanical characterization of a viscoelastic material, can be understood in the case of oscillatory temperature loads that act on the body when the material properties continuously change due to temperature.

Let's consider an example: when two different types of loads act on the viscoelastic body simultaneously, at different loading rates, they produce two different stresses,  $\sigma_1(t)$  and  $\sigma_2(t)$ . Since the loads are of different types, the strain rates are also different. Therefore, although it is the same propellant, the tensile strengths  $\sigma_{m1}(t)$  and  $\sigma_{m2}(t)$  that correspond to different loads are also different, because they depend on the strain rate. Then, the effects of individual loads have to be analyzed separately, using the concept of convolution [7] which is valid for linear-viscoelastic materials. Each of them creates a certain current damage, because it occupies a part of the total capacity of viscoelastic material to withstand loads. The first current damage is equal to the ratio between the first stress  $\sigma_1(t)$  and the first tensile strength  $\sigma_{m1}(t)$ . The same principle applies to the second load. The values of current damages represent the ratios between real stresses and their appropriate ultimate stresses.

In the case considered, the effect of two loads can be represented as the sum of two damage increments, similar to the principle that is used in the Miners cumulative damage law [30]:

$$\begin{aligned} d(t) &= d_1(t) + d_2(t) = \frac{\sigma_1(t)}{\sigma_{m1}(t)} + \frac{\sigma_2(t)}{\sigma_{m2}(t)} = \\ &= \frac{\sigma_1(t)}{(\sigma_{m1})_0 \eta_\sigma(t)} + \frac{\sigma_2(t)}{(\sigma_{m2})_0 \eta_\sigma(t)} \end{aligned} \tag{28}$$

The sum of several individual damages represents the total damage. The possible question could be whether this is just a simple sum of the minor current damages or such amount has to be determined by a geometric principle. It should be a matter of structural analysis.

According to the terminology adopted in the theory of elasticity, the reciprocal of the total damage corresponds to the safety factor of the body.

$$\nu(t) = \frac{1}{d(t)} \quad (29)$$

The above example shows that, unlike elastic material, for the analysis the reliability of a viscoelastic body, it is necessary to make all functional dependences of viscoelastic mechanical properties on temperature and strain rate.

### The basic viscoelastic mechanical properties and further required measurements

During the uniaxial mechanical characterization of the composite rocket propellant presented here, the first members of the expressions (6)–(8) are determined: tensile strength ( $\sigma_{m0}$ ), strain at maximum stress (allowable strain) ( $\varepsilon_{m0}$ ), and relaxation modulus ( $E_{rel0}$ ). Based on these results, safety factor of an arbitrary viscoelastic body can be determined at the initial moment of its service life. It is sometimes enough.

In addition, further mechanical characterization as an input for structural analysis of a viscoelastic body should include deterioration of mechanical properties due to the natural aging and the changes due to the cumulative damage.

The effect of natural aging is reflected through the aging factors ( $\eta$ ) in expressions (6)–(8). These factors differ for different mechanical properties of materials. For a complete structural analysis it is necessary to define the values of these factors. Changes of the mechanical properties due to the natural aging can be very large in the initial period after the process of polymer curing [10,20,31,32]. An example of the aging factor time-dependence over the period of three years, for the ultimate strain of an HTPB propellant [8,11] is shown in Fig. 18. It indicates an important aging influence, especially in the initial period of the service life.

The initial values of the mechanical properties of viscoelastic materials are displayed as master curves, which represent their functional dependences on temperature and strain rate.

When the changes due to real time are introduced in the form of simple aging functions, in the manner as in expressions (6)–(8), it means that the master curves translationally move through the real aging time, without changing the relations between temperature and strain rate. Otherwise, the master curve could change

their shapes and slopes. At first, it is not possible to estimate in advance whether the influences of temperature and strain rate on the mechanical properties change due to aging in different manners. Second, the abscissas of the master curves have time dimensions, as reciprocals of the strain rate effects. But is there a difference between the impact of real aging-time and strain rate? This dilemma was discussed in the second series of tests in this paper. In Figs. 15–17 the regression curves of modulus, tensile strength and ultimate strain are parallel in all cases for two different time points in an interval of 3 months. Their displacements along the horizontal line (timeline) would lead to their approximate overlap. This means that between the same strain rates in two different time points the horizontal distances are the same, regardless to the values of strain rates. Aging time didn't disrupt the allocation of different strain rate points at the standard temperature. This means intuitively that it was possible to carry out these tests in other circumstances, not only standard conditions (20 °C, 50 mm/min). The same results would probably have been obtained. The conclusion of this review is as follows: due to the natural aging, master curves of the mechanical properties move translationally along the curves represented by the time-distribution of the aging factors.

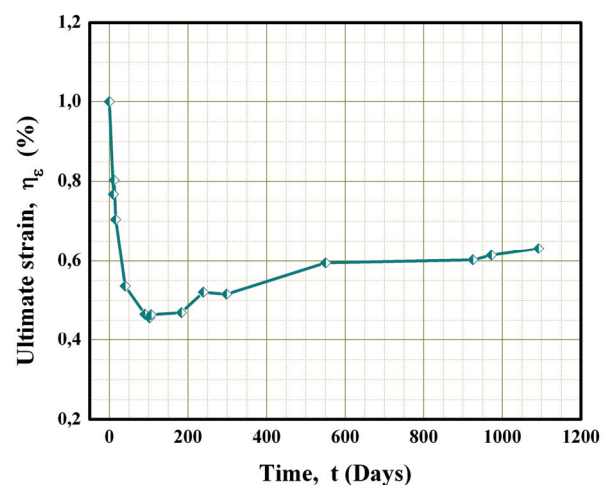


Figure 18. Ultimate strain aging factor.

The effect of cumulative damage is usually neglected because it is less influential at the beginning of service life [6,7]. Some authors believe that cumulative damage becomes significant after a lengthy storage period [12,13,29] or perhaps even earlier [33] but not at the beginning of service life. However, in the Rocket Armament Department in MTI it has been shown in the case of anti-hail propellant grain [10] that this impact can be very large at the beginning of the propellant service life, and shouldn't be neglected.

**CONCLUSION**

Very often, in engineering practice, structural analysis of viscoelastic materials is done superficially, similar to an elastic material. Despite many papers dealing with this subject, safety factor for a viscoelastic body is sometimes determined based on the data measured under standard conditions (20 °C, tester cross-head speed 50 mm/min). Such a result is often not accurate and gives a completely wrong conclusion about the reliability of the body. During mechanical loading, viscoelastic material behaves quite differently compared to an elastic material. It is not possible to determine the safety factor or reliability of a viscoelastic body without detailed mechanical characterization of the viscoelastic material, because its mechanical properties depend on temperature and strain rate, as well on its age and load history. Therefore, it is also important to carry out the load analysis. Concentrated forces, pressure, acceleration of the body or environmental temperature have completely different effects on the viscoelastic material. Therefore it is necessary to know the behavior of the viscoelastic material in all load conditions.

The principles of test data processing of the mechanical properties of viscoelastic materials are generally known in literature. However, it is almost impossible to find a detailed overview of the data processing. This paper presents an example of simple uniaxial mechanical testing of a composite rocket propellant, as an approximately linear-viscoelastic material. A method of processing constant strain rate tension tests data is presented, in order to obtain the input for the structural analysis of a rocket motor propellant grain reliability and its service life.

In this paper it is also shown that, when a complete mechanical characterization of a viscoelastic material is made in an arbitrary time point, further it is sufficient only to monitor the time distribution of the mechanical properties only in standard test conditions.

Finally, the composite rocket propellant maybe does not have wide application, except in missile technology, but other viscoelastic materials are widely used in engineering practice. The procedure and test results presented in this paper, can be useful as a starting point for analysis of some similar linear-viscoelastic materials.

**Nomenclature**

$A_0$	Initial specimen cross-section, $\text{cm}^2$
$A, B, C, D, C_1, C_2$	Constants
$a, b, c, d$	Constants
$a_T$	Time–temperature shift factor
$D, D(t)$	Cumulative damage, time-dependent cumulative damage

$d, d(t)$	Damage, time-dependent current damage
$E, E_e, E_{rel}$	Modulus, equilibrium modulus, relaxation modulus, $\text{daN}/\text{cm}^2$
$E_0$	Initial modulus, $\text{daN}/\text{cm}^2$
$E_i$	Constant in the Relaxation modulus expression, $\text{daN}/\text{cm}^2$
$E(\omega)$	Dynamic modulus, $\text{daN}/\text{cm}^2$
$E'(\omega), E''(\omega)$	Storage modulus, Loss modulus, $\text{daN}/\text{cm}^2$
$F$	Force, $\text{daN}/\text{cm}^2$
$l_0$	Effective specimen length, mm
$O_1, O_2$	Differential operators
$P_i, Q_i$	Constants
$R$	Strain rate
$T, T_0, T_R$	Temperature, reference temperature, °C
$T_p$	Glass transition temperature, °C
$t$	Time, s
$V$	Tensile tester cross-head speed, mm/min
$\Delta$	Increment
$\varepsilon, \varepsilon_0$	Strain, Initial strain, %
$\varepsilon_m, \varepsilon_{m0}, \varepsilon_m(t)$	Ultimate (allowable) strain, initial, time dependent, %
$\varepsilon_{RED}$	Reduced strain, %
$\dot{\varepsilon} = d\varepsilon / dt$	Strain rate, $\text{s}^{-1}$
$\xi$	Reduced time, s
$\eta(t)$	Propellant aging factor
$\eta_E, \eta_\sigma, \eta_\varepsilon$	Aging factor for modulus, stress, strain
$V, V_\sigma, V_\varepsilon$	Safety factor, safety factors based on stress and strain criteria
$\sigma, \sigma_m$	Stress, strength (ultimate stress), $\text{daN}/\text{cm}^2$
$\sigma_{m0}, \sigma_m(t)$	Initial strength, time-dependent strength, $\text{daN}/\text{cm}^2$
$\sigma_{RED}$	Reduced stress, $\text{daN}/\text{cm}^2$
$\tau_i$	Relaxation times, s
$\omega$	Circular frequency, Hz

**Acknowledgments**

The authors would like to thank MTI's Sector for materials and protection (Composite rocket propellant department), which has produced propellant specimens and provided logistics for testing, as well as the financial support of the project TR 36050 (Research and development of unmanned aircraft in support of traffic infrastructure monitoring).

**REFERENCES**

[1] M.L. Williams, P.J. Blatz, R.A. Schapery, Fundamental Studies Relating to Systems Analysis of Solid Propellants, Final report GALCIT 101, Guggenheim Aero. Lab., Pasadena, CA, 1961.

- [2] V. Rodić, M. Petrić, The effect of curing agents on solid composite rocket propellant characteristics, *Scientific Technical Review*, LV (2005) 46–50.
- [3] S. Brzić, Lj. Jelisavac, J. Galović, D. Simić, J. Petković, Viscoelastic Properties of hydroxyl-terminated poly (butadiene) – based composite rocket propellants, *Hem. Ind.* **68** (2014) 435–443.
- [4] M.L. Williams, Structural Analysis of Viscoelastic Materials, *AIAA J.* (1964) 785–798.
- [5] R.F. Landel, T.L. Smith, Viscoelastic Properties of Rubberlike Composite Propellants and Filled Elastomers, *ARS J.* **31** (1960) 599–608.
- [6] J.E. Fitzgerald, W.L. Hufferd, Handbook for the Engineering Structural Analysis of solid Propellants, CPIA publication 214, 1971.
- [7] Solid propellant grain structural integrity analysis, NASA Space Vehicle Design Criteria SP–8073, 1973.
- [8] N. Gligorijević, Strukturna analiza pogonskih punjenja raketnih motora sa čvrstim gorivom, Vojnotehnički Institut Beograd, 2013.
- [9] N. Gligorijević, Prilog strukturnoj analizi vezanog pogonskog punjenja raketnog motora sa čvrstom pogonskom materijom, Magistarski rad, Mašinski fakultet u Beogradu, , 1989.
- [10] N. Gligorijević, S. Živković, V. Rodić, S. Subotić, I. Gligorijević, Effect of Cumulative Damage on Rocket Motor Service Life, *J. Energ. Mater.* **33** (2015) 229–259.
- [11] N. Gligorijević, V. Rodić, R. Jeremić, S. Živković, S. Subotić, Structural Analysis Procedure for a Case Bonded Solid Rocket Propellant Grain, *Sci. Tech. Rev.* **61** (2011) 1–9.
- [12] R.A. Heller, M.P. Singh, Thermal Storage Life of Solid–Propellant Motors, *J. Spacecraft Rockets* **20** (1983) 144–149.
- [13] R.A. Heller, M.P. Singh, H. Zibdeh, Environmental Effects on Cumulative Damage in Rocket Motors, *J. Spacecraft Rockets* **22** (1985) 149–155.
- [14] G.P. Sutton, O. Biblarz, *Rocket Propulsion Elements*, 7<sup>th</sup> ed., Wiley, New York, 2001.
- [15] N. Gligorijević, S. Živković, S. Subotić, S. Kozomara, M. Nikolić, A. Boulahlib, Solving an Irregular Burning Problem in a Small Rocket Motor, *Sci. Tech. Rev.* **64** (2014) 1–11.
- [16] Structural Assessment of Solid Propellant Grains, Agard Advisory Report 350, 1997.
- [17] C.T. Liu, Cumulative Damage and Crack Growth in Solid Propellant, Media Pentagon Report No. A486323, 1997.
- [18] S. Cerri, A.M. Bohn, K. Menke, L. Galfetti, Ageing Behavior of HTPB Based Rocket Propellant Formulations, *Cent. Eur. J. Energ. Mat.* **6** (2009) 149–165.
- [19] N. Gligorijević, Istraživanje pouzdanosti i veka upotrebe raketnih motora sa čvrstom pogonskom materijom (Solid propellant rocket motor reliability and service life research), Ph.D. Thesis, Military Academy, Belgrade, Serbia, 2010.
- [20] N. Gligorijević, S. Živković, S. Subotić, B. Pavković, M. Nikolić, S. Kozomara, V. Rodić, Mechanical Properties of HTPB Propellants in the Initial Period of Service Life, *Sci.Tech. Rev.* **64** (2014) 1–13.
- [21] В.В. Москвитин, Сопротивление вязко-упругих материалов, Наука, Москва, 1972.
- [22] N. Gligorijević, S. Živković, S. Subotić, S. Kozomara, M. Nikolić, S. Čitaković, Side Force Determination in the Rocket Motor Thrust Vector Control System, *Sci.Tech. Rev.* **63** (2013) 27–38.
- [23] K.W. Bills Jr., J.H. Wiegand, Relation of Mechanical Properties to Solid Rocket Motor Failure, *AIAA J.* **37** (1964) 524–541.
- [24] M.L. Williams, R.F. Landel, J.D. Ferry, The Temperature Dependence of Relaxation Mechanisms in Amorphous Polymers and Other Glass-forming Liquids, *J. Am. Chem. Soc.* **77** (1955) 3701–3707.
- [25] N. Gligorijević, V. Rodić, Determination of solid propellant modulus in the process of propellant grain structural analysis, International Symposium on defense technologies, Belgrade, MTI, OTEH, 2009.
- [26] D.J. Ferry, *Viscoelastic Properties of Polymers*, 3<sup>rd</sup> ed., Wiley, New York, 1980.
- [27] D.I. Thrasher, J.H. Hildreth, Structural Service Life Estimate for a Reduced Smoke Rocket Motor, *J. Spacecraft Rockets* **19** (1982) 564–570.
- [28] L.D. Villar, T. Cicaglioni, M.F. Diniz, M.F.K. Takahashi, L.C. Rezende, Thermal aging of HTPB/IPDI-based polyurethane as a function of NCO/OH ratio, *Mater. Res.* **14** (2011) 372–375.
- [29] H.S. Zibdeh, R.A. Heller, Rocket Motor Service Life Calculations Based on the First Passage Method, *J. Spacecraft Rockets* **26** (1989) 279–284.
- [30] M.A. Miner, Cumulative Damage in Fatigue, *J. Appl. Mech-t Asme* **12** (1945) 159–164.
- [31] L. Gottlieb, S. Bar, Migration of plasticizer between Bonded Propellant Interfaces, *Propell. Explos. Pyrot.* **28** (2003) 12–17.
- [32] H. Shekhar, D.A. Sahasrabudhe, Assessment of Poissons Ratio for Hydroxy-terminated Polybutadiene-based Solid Rocket Propellants, *Defence Sci. J.* **60** (2010) 497–501.
- [33] S. Woei Chyuan, A study of loading history effect for thermoviscoelastic solid propellant grains, *Comput. Struct.* **77** (2000) 735–745.



**ИЗВОД****МЕХАНИЧКА КАРАКТЕРИЗАЦИЈА КОМПОЗИТНОГ ЧВРСТОГ РАКЕТНОГ ГОРИВА НА БАЗИ ХИДРОКСИ-ТЕРМИНИРАНОГ ПОЛИБУТАДИЕНА**

Никола И. Глигоријевић, Весна Ж. Родић, Саша Ж. Живковић, Бојан М. Павковић, Момчило М. Николић, Стеван М. Козомара, Средоје Д. Суботић

*Војнотехнички Институт, Рајка Ресановића 1, Београд*

(Научни рад)

У раду је приказана процедура обраде података једноосне механичке карактеризације композитног чврстог ракетног горива на бази хидрокси-терминираних полибутадиена, као линеарно-вискоеластичног материјала чије механичке особине изразито зависе од температуре и брзине деформације. Разматран је поступак припреме података у облику који је потребан за структурну анализу вискоеластичног тела и процену степена сигурности и поузданости. Епрувете горива су испитиване истезањем константним брзинама клема кидалице, на 96 различитих режима који су обухватили по 12 различитих температура и брзина клема. Приказан је поступак одређивања фактора температурско-временске корекције. Показан је и начин израде јединствених дијаграма зависности механичких особина горива од редукованог времена као величине која обухвата истовремени утицај температуре и брзине деформације. Израђене су тзв. „мастер криве“ затезне чврстоће, дозвољене деформације, иницијалног модула и модула релаксације горива које важе у свим условима оптерећења. Функционалне зависности ових величина представљају улазне податке за структурну анализу и представљене су у математичком облику, погодном за даљу анализу. Овај начин обраде података може да се примени на било које тело од вискоеластичног материјала. Разматране су неке разлике у приступу структурној анализи вискоеластичног и еластичног тела. На једном примеру је показана потреба израде података у облику „мастер кривих“, које показују зависност механичких особина у широком спектру услова оптерећења. Особине ракетног горива могу да послуже као узорак при разматрању неког другог вискоеластичног материјала. У раду су разматране механичке карактеристике горива које одговарају почетном периоду употребе, одмах након израде, када нема утицаја старења или акумулације оштећења услед дејства спољних оптерећења. Ове почетне величине су углавном довољне за процену основне (почетне) поузданости вискоеластичног тела, која се касније мења током времена. Приказан је и поступак праћења утицаја природног старења и извршена експериментална анализа исправности овог поступка. За комплетну структурну анализу и процену века трајања потребне су и вредности фактора акумулације оштећења, које овде нису разматране, јер зависе од реалних услова оптерећења.

*Кључне речи:* Гориво композитно • Вискоеластичност • Механичка карактеризација • Затезна чврстоћа • Дозвољена деформација • Температурско–временска корелација • Модул релаксације • Степен сигурности • Редуковано време